



Highly active mixed-phase TiO₂ photocatalysts fabricated at low temperature and the correlation between phase composition and photocatalytic activity

SHI Lei, WENG Duan*

Laboratory of Advanced Materials, Department of Materials Science and Engineering, Tsinghua University, Beijing 100084, China.
E-mail: sl01@mails.thu.edu.cn

Received 28 November 2007; revised 4 January 2008; accepted 9 January 2008

Abstract

The idea of varying volume ratio of water to ethanol in solvent was firstly employed to yield phase composition controllable mixed-phase titanium dioxide (TiO₂) photocatalysts via a low temperature solvothermal route at 353 K. It was found that anatase contents increase from 0 to 100% with increase of ethanol contents in solvent. The mixed-phase TiO₂ with 60% anatase content exhibited the best photocatalytic activity in photodecomposing formaldehyde (FAD) under UV light irradiation, which increases by about 270 or 400% in comparison with single rutile or anatase TiO₂, and is slightly better than commercial mixed-phase TiO₂ (P25). The synergistic effect in mixed-phase TiO₂ including antenna effect by rutile phase and the activation effect by anatase phase was observed. Further, partially quantitative correlation between phase composition and photocatalytic activity was ascribed to maximizing the synergistic effect and an optimal value of anatase content about 60% in mixed-phase TiO₂ photocatalyst was therefore suggested.

Key words: titanium dioxide; solvothermal synthesis; phase compositional control; synergistic effect; photocatalysis

Introduction

Most people spend as much as 90% of their time indoors, so volatile organic compounds (VOCs) released from buildings and furnishing may pose a greater threat to health than those in outdoor air do. In particular, formaldehyde (FAD) pollutant has significant harmful effects to human health and may cause some diseases of the respiratory tract, even leukemia and cancers. Titanium dioxide (TiO₂), owing to its excellent photocatalytic activity, high stability against photocorrosion, and nontoxicity, has been widely investigated as a kind of promising photocatalysts to remove various organic pollutants in water or air since 1970s (Ollis, 1985).

To achieve higher photocatalytic activity of TiO₂, some optimization work has been done, including the control over size, morphology, and microstructure (Chen and Mao, 2007). In particular, previous work found that mixed-phase TiO₂ photocatalysts, for example, commercial Degussa P25 powder (ca. 25% rutile and 75% anatase), had higher photocatalytic activities than those in single anatase or rutile phase, which was ascribed to synergistic effect between the two phases (Ohno *et al.*, 2001). Further characterizations by EPR method affirmed the electron transfer between the two phases and suggested phase composition to be a fundamentally important factor in high photocat-

alytic activity (Hurum *et al.*, 2005). Recently, systematical solvothermal preparation and characterization researches on phase-compositional control over TiO₂ nanoparticles were published (Testino *et al.*, 2007), implying that compositional control over TiO₂ via solvothermal method are receiving growing interests. However, there are still two shortcomings in this route. One is the change of phase composition does not exhibit good regularity. The other is that the synthetic route is not facile enough owing to its wide synthetic temperature range and brookite TiO₂ can be observed at low synthetic temperature. Besides, till now, the quantitative correlation between phase composition and photocatalytic activity has not been clarified yet.

Driven by realizing phase compositional control over TiO₂ (only rutile and anatase phases) at low temperature and seeking for correlation between phase composition and photocatalytic activity, herein, a systematic low temperature solvothermal route were developed to synthesize phase composition controllable mixed-phase TiO₂ at 353 K by varying the solvent composition. The characterization of physicochemical properties and the evaluation of photocatalytic activity were performed to elucidate the nature of synergistic effect between the rutile and anatase phases. Further, the partially quantitative correlation between phase composition and photocatalytic activity and the optimal anatase content in mixed-phase TiO₂ photocatalysts was suggested according the data of photocatalysis.

* Corresponding author. E-mail: duanweng@mail.thu.edu.cn.

1 Materials and methods

1.1 Preparing mixed-phase TiO₂

TiCl₃ (15%–20% solution), HNO₃ (65%–68% solution), ethanol (≥ 99.7%) and urea (≥ 99.0%) were purchased from Beijing Beihua Fine Chemical Co., Ltd. as analytical reagents and used without further purification. Typically, 0.4 ml of 10 mol/L HNO₃ was added to a 20-ml 15%–20% TiCl₃ solution. The color of the solution changed to light green and then gold yellow as a consequence of the oxidation of Ti³⁺ to Ti⁴⁺. Then, 6 g urea was added to the solution to adjust the molar ratio of Ti⁴⁺ to urea to 1:4. Five oxidized TiCl₃ solutions were diluted by 40 ml solvent (referred to as dilution solvent) with various volume ratios of water to ethanol (40:0, 30:10, 20:20, 10:30, and 0:40, denoted as sample 1 to 5 below) and placed into five Teflon-lined stainless steel autoclaves with an internal volume of 100 ml. Followed by heating at 353 K for 24 h under autogenous pressure, TiO₂ particles were precipitated from the solutions. Finally, the yielded off-white products were filtered, washed thoroughly using distilled water and ethanol successively, and dried in vacuum at 333 K for 24 h prior to being characterized.

1.2 Evaluation of photocatalytic activity

To simulate the practical application condition, in which buildings and furnishing may continuously release VOCs, photocatalytic activities of samples were evaluated in a continuous flow photoreactor under UV light irradiation using FAD as target organic. The experimental configuration and process were adapted from the literature (Zhang et al., 2006). In detail, 50 mg sample was dispersed in 2 ml ethanol by ultrasonic treatment for 10 min. Then, the obtained suspension was dripped onto the glass slide with an area of (7.5 cm × 2.5 cm, length × width) to spread the powders uniformly and the coated glass slide was dried in air for 12 h prior to being placed into the quartz vessel. UV-light lamp of 11 W (Institute of Electric Light Source, Beijing) was used to provide UV light irradiation. The vertical distance between the glass slide and the lamp was 10 cm, where the values of light intensity at the wavelengths of 254, 297, 365, and 400 nm were 2.7, 2.1, 2.1, and 0.4 mW/cm, respectively. The inlet gas flow was mixed of air and FAD at a flow rate of 50 and 10 ml/min, respectively. During the photodecomposition process, the temperature of the photoreactor was maintained at 293 K. The concentrations of FAD and possible intermediate products in the outlet gas flow were traced by gas chromatograph (SP-502, Lunan Chemical Instrument Co., Ltd., China) operating with a flame ionization detector (FID) and a 2-m stainless steel column (GDX-403) at 373 K.

2 Results and discussion

2.1 Physicochemical properties of mixed-phase TiO₂ photocatalysts

Figure 1 shows the XRD patterns (D/max-2500, 40 kV, 200 mA, Rigaku, USA) of sample 1 to 5. The standard

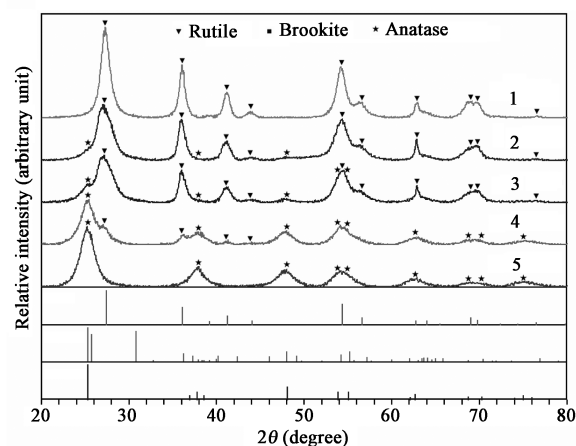


Fig. 1 XRD patterns of sample 1 to 5 yielded via solvothermal process at 353 K for 24 h by varying the volume ratios of water to ethanol in dilution solvent: (1) 40:0, (2) 30:10, (3) 20:20, (4) 10:30, (5) 0:40.

diffraction data from JCPDS files of anatase (No. 21-1272), rutile (No. 21-1276), and brookite (No. 29-1360) are also given to identify phase composition. As shown in Fig.1, the increase of ethanol content in dilution solvent obviously leads to the increase of anatase content in the mixed-phase TiO₂ particles. In particular, no brookite phase can be observed. For quantitative comparison, Table 1 summarizes the parameters of each sample, including the volume ratios of water to ethanol in dilution solvent, weight fraction of anatase phase (denoted as x_a) and crystallite size. The values of x_a were calculated by the following equation:

$$x_a = \frac{0.884I_A}{0.884I_A + I_R}$$

where, I_A and I_R are the integrated intensities of anatase (101) and rutile (110) peaks (Zhang and Banfield, 2000). In addition, the average crystallite sizes were also calculated by Scherrer's equation. As shown in Table 1, with increase of ethanol contents in dilution solvent, the values of x_a consistently increase from 0 to 1.0 and crystallite sizes of rutile and anatase phases consistently decrease from 11.9 to 4.91 nm and from 6.38 to 4.73 nm, suggesting that higher ethanol contents prefer to form anatase phase and inhibit gain of crystallite sizes of both phases.

Because TiO₂ can only absorb the UV light corresponding to the wavelength shorter than 420 nm, Fig.2 shows the diffuse reflection spectra (UV-3010, Hitachi, Japan) of the

Table 1 Dilution solvent compositions and parameters of the yielded TiO₂ particles

Sample	Dilution solvent ^a	Weight fraction of anatase ^b	D^c (nm)
1	40:0	Rutile, $x_a = 0$	11.9 (R)
2	30:10	Anatase + rutile, $x_a = 0.0471$	6.38 (A), 6.31 (R)
3	20:20	Anatase + rutile, $x_a = 0.0932$	5.53 (A), 6.06 (R)
4	10:30	Anatase + rutile, $x_a = 0.589$	4.82 (A), 4.91 (R)
5	0:40	Anatase + rutile, $x_a \approx 1.00$	4.73 (A)

^a Volume ratios of water to ethanol in 40 ml dilution solvent; ^b x_a denotes the weight fraction of anatase in synthesized samples; ^c crystalline sizes of anatase and rutile phases. Anatase is denoted as (A) and rutile as (R), similarly.

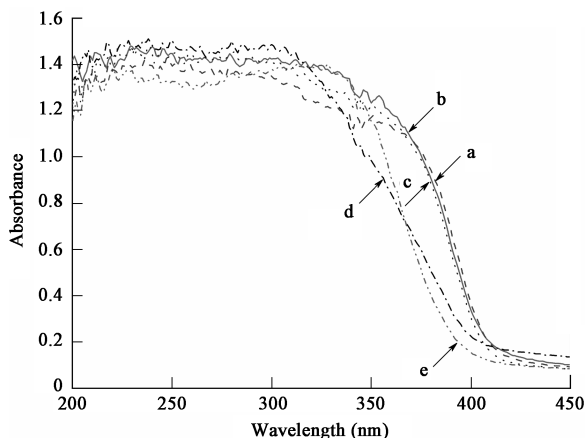


Fig. 2 UV-Vis diffusion reflectance spectra of the yielded TiO₂ samples. (a) sample 1; (b) sample 2; (c) sample 3; (d) sample 4; (e) sample 5.

yielded TiO₂ samples in the range of wavelengths from 200 to 450 nm. It is obvious that the yielded TiO₂ samples have similar photoabsorption in the range of wavelengths from 200 to 350 nm. Besides, the absorption edges of the yielded TiO₂ samples from sample 1 to 5 occur at 412, 411, 410, 403, and 390 nm, and accordingly the band gap energies are estimated to be about 3.00, 3.01, 3.02, 3.08, and 3.17 eV, respectively. The band gap energies of single rutile and anatase phases are consistent with the reported values (Lee *et al.*, 2005), and the gradual increase of band gap energies is in good agreement with increase of anatase contents in mixed-phase TiO₂. Since crystallite sizes of the yielded TiO₂ samples are in a small range from 4.73 to 6.38 nm except sample 1, only tiny changes in band gap energies are introduced by quantum size effect. Considering the difference in band gap energies, results here revealed that higher rutile content leads to a stronger photoabsorption in the range of wavelengths from 350 to 450 nm.

2.2 Photocatalytic activities of yielded TiO₂ photocatalysts

Figure 3 shows the plots of $C/C_0 \times 100$ versus photodecomposition time, where C and C_0 are the concentrations of FAD in the outlet flow at the time t and at the initial equilibrium state, using P25 as reference. The initial

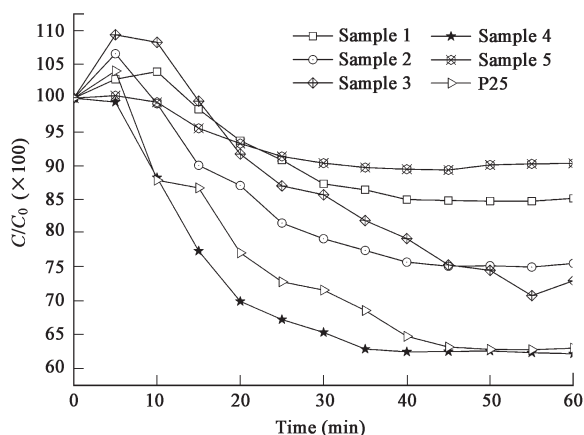


Fig. 3 $C/C_0 \times 100$ versus photodecomposition time, using Degussa P25 as a reference catalyst.

equilibrium state was obtained by maintaining the inlet gas flow for 1 h before turning on UV light irradiation. As shown in Fig.3, the values of $C/C_0 \times 100$ go up at the beginning except sample 4, implying that an intensive desorption of FAD from TiO₂ particles occurs upon turning on the UV light irradiation. All samples reach the final equilibrium state after 60 min, at which a lower value of $C/C_0 \times 100$ corresponds to a higher concentration of photodecomposed FAD. The order of photocatalytic activities is: sample 4 > sample 3 > sample 2 > sample 1 > sample 5, and the corresponding anatase contents are 60%, 10%, 5%, 0, and 100%. This result indicates that photocatalytic activities of the yielded mixed-phase TiO₂ particles gradually increase as the increase of anatase content. The photocatalytic activity of sample 4 increases by about 270% and 400% in comparison with single rutile and anatase TiO₂ and is a little superior to that of commercial Degussa P25, suggesting that current solvothermal route is a promising low temperature route to fabricate highly active TiO₂ photocatalysts.

2.3 Heterogeneous reaction mechanism of photodecomposing FAD

According to the gas chromatography charts of obtained samples, formic acid is found to be the only intermediate of photodecomposing FAD. This result is consistent with previous literature and the relevant free radical reactions are listed as follows, implying that the formation of formic acid mainly leads to the consumption of hydroxyl free radicals (Reactions (1)–(4)) (Yang *et al.*, 2000):

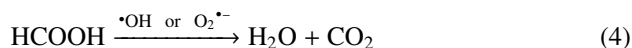
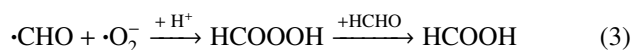
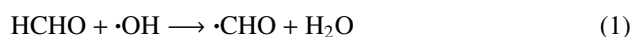


Figure 4 shows the plots of concentration of formic acid (denoted as C_{HCOOH}) versus time from 0 to 60 min, using P25 as reference. The values of C_{HCOOH} for each sample go up at the beginning and then gradually decrease to a stable value at the final equilibrium state (denoted as

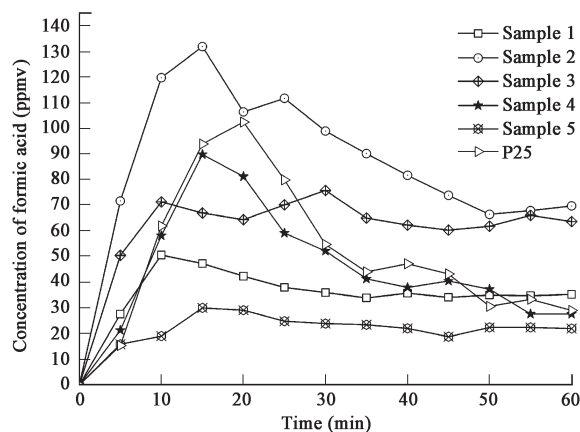


Fig. 4 Concentrations of formic acid of the yielded TiO₂ samples versus time from 0 to 60 min using P25 as reference.

$\text{C}_{\text{HCOOH}}^{\cdot}$), which corresponds to the formation and further decomposition of formic acid according to Reactions (1)–(4). As shown in Fig.4, the value of $\text{C}_{\text{HCOOH}}^{\cdot}$ for sample 2 (ca. 70 ppmv) increases by about 100% in comparison with sample 1 (ca. 35 ppmv), indicating that the formation rate of formic acid can be accelerated by the presence of about 0.05 wt fraction of anatase phase in rutile TiO_2 . The value of $\text{C}_{\text{HCOOH}}^{\cdot}$ for sample 3 is about 63 ppmv, which increases by about 80% in comparison with sample 1 and decreases by about 10% in comparison with sample 2. Furthermore, the values of $\text{C}_{\text{HCOOH}}^{\cdot}$ for sample 4 and P25 (ca. 28 ppmv) are even smaller than that for sample 1. Combined with the photocatalytic activities as indicated in Fig.4, the decrease of the values of $\text{C}_{\text{HCOOH}}^{\cdot}$ with the increase of anatase contents can only be ascribed to the faster decomposition rate of formic acid. Therefore, it can be deduced here that the anatase phase in rutile TiO_2 not only accelerates the formation rate of formic acid, but also efficiently accelerates the decomposition rate of formic acid. In addition, rutile phase is observed to have a faster rate of forming formic acid than anatase phase.

2.4 Correlation between phase composition and photocatalytic activity

Considering the consistency of photocatalytic activities and phase compositions, higher photocatalytic activities of mixed-phase TiO_2 can be ascribed to the synergistic effect. On one hand, as confirmed in Fig.2, the stronger photoabsorption of rutile phase in the range of wavelengths from 350 to 450 nm provides more probabilities to promote electrons from valence band into conductive band, which is favorable to produce more electron-hole pairs and hence to form more active hydroxyl and oxygen anion free radicals. This can be considered as the antenna effect by rutile phase. On the other hand, in mixed-phase TiO_2 , the electron transfer from rutile to anatase phase can reduce the recombination of photogenerated charges. As shown in Fig.5a, because the conductive band of anatase phase locates at a higher energy position than that of rutile phase by about 0.20 eV, previous work considered that the electron transfer was driven by thermal activation (Ohno *et al.*, 2003). In this work, partial drive of electron transfer can be ascribed to the surface band bending, which has already been observed in photosplitting water and proved by surface photovoltage spectroscopy (Jing *et al.*, 2003). Since rutile TiO_2 has a stronger photoabsorption than anatase TiO_2 , there will be more photogenerated carriers in it. For the photocatalysis following free radical mechanism, hydroxyl free radicals are formed by oxidating hydroxyl groups with photogenerated holes. According to the mechanism of photodecomposing FAD, more hydroxyl free radicals are consumed during the formation of formic acid, suggesting that more photogenerated holes are consumed. Combined with its faster rate of forming formic acid than anatase phase, more photogenerated electrons will temporarily accumulate in rutile TiO_2 . As shown in Fig.5b, this accumulation of electrons leads to a bigger bending (upward shift) of conductive band in rutile phase than that in anatase phase and makes the electron transfer

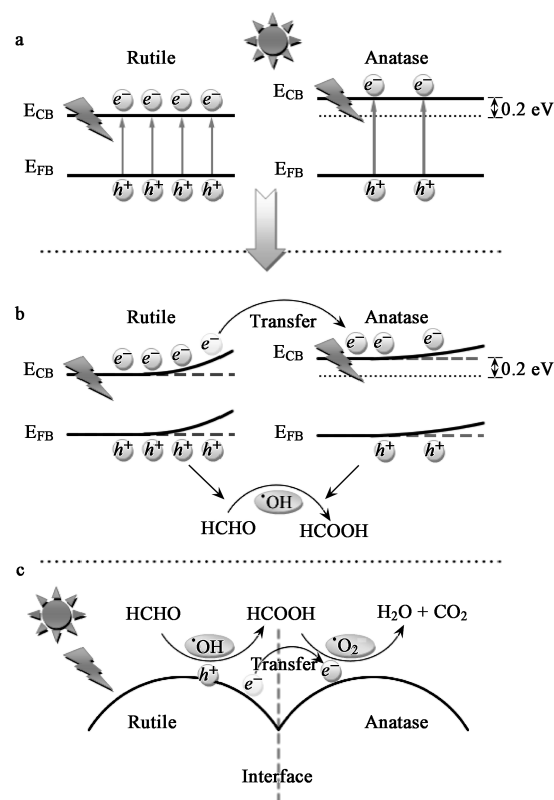


Fig. 5 Scheme of the drive of electron transfer and relative photocatalysis reactions. (a) Bands positions of rutile and anatase phases; (b) the surface bands bending of rutile and anatase phases during photodecomposing FAD; (c) the adsorption of formic acid molecule by oxygen anion free radicals on the surface of anatase phase.

from rutile to anatase feasible as expected. After the electron transfer from rutile to anatase phase, oxygen anion free radicals are formed on the surface of anatase phase as shown in Fig.5c. Due to their strong Lewis base characteristics, formic acid molecule can be adsorbed more easily on anatase phase. The electron transfer not only inhibits the recombination of photogenerated charges, but also is favorable for formic acid to be further oxidized. This can be considered as the activation effect by anatase phase. Therefore, the correlation between phase composition and photocatalytic activity can be ascribed to maximizing the synergistic effect in mixed-phase TiO_2 . According to the photocatalytic activities, low anatase content is not sufficient to maximize the activation effect as indicated by comparing samples 2 and 3 with sample 4, while high anatase content is disadvantageous to the antenna effect by rutile phase as indicated by comparing sample 5 with sample 4. In addition, commercial P25 (70% anatase content) has the higher crystallinity and the bigger crystalline size (about 25 nm) in comparison with sample 4. If the two opposite factors are considered to be counteracted, it can be deduced here that the 60% anatase content might be an optimal anatase content in mixed-phase TiO_2 .

3 Conclusions

Via low temperature solvothermal process at 353 K, phase compositional control over TiO_2 was realized and

the anatase contents in yielded TiO₂ particles were found to increase monotonically from 0 to 100% with the increase of ethanol content in solvent. Highly active mixed-phase TiO₂ (sample 4, ca. 60% anatase) is yielded, whose photocatalytic activity increases by about 270% or 400% in comparison with yielded single rutile or anatase TiO₂ and is even a little superior to that of commercial Degussa P25. Its high photocatalytic activity is ascribed to the synergistic effect consisting of the antenna effect by rutile phase and the activation effect by anatase phase. The partial drive of electron transfer from rutile phase to anatase phase is deduced to be the origin of surface band bending. Therefore, the partially quantitative correlation between phase composition and photocatalytic activity is considered to maximize the synergistic effect and an optimal anatase content of about 60 wt.% is suggested. Current solvothermal route not only reduces the energy consumption for the fabrication of mixed-phase TiO₂ but also might extend the utilization of TiO₂ photocatalysts at low temperature. Our further studies are aimed at using the yielded mixed-phase TiO₂ as precursors to synthesize metal or nonmetal doped mixed-phase photocatalysts for visible light driven photocatalysis.

Acknowledgments

This work was supported by the Ministry of Science and Technology, China (No. 2004CB719503).

References

- Chen X, Mao S S, 2007. Titanium dioxide nanomaterials: synthesis, properties, modifications, and applications. *Chem Rev*, 107: 2891–2959.
- Hurum D C, Gray K A, Rajh T, Thurnauer M C, 2005. Recombination pathways in the Degussa P25 formulation of TiO₂: Surface versus lattice mechanisms. *J Phys Chem B*, 109: 977–980.
- Jing L Q, Sun X J, Shang J, Cai W M, Xu Z L, Du Y G, Fu H G, 2003. Review of surface photovoltage spectra of nano-sized semiconductor and its applications in heterogeneous photocatalysis. *Sol Energ Mat Sol C*, 79: 133–151.
- Lee H S, Woo C S, Youn B K, Kim S Y, Oh S T, Sung Y E, Lee H I, 2005. Bandgap modulation of TiO₂ and its effect on the activity in photocatalytic oxidation of 2-isopropyl-6-methyl-4-pyrimidinol. *Top Catal*, 35: 255–260.
- Ohno T, Tokieda K, Higashida S, Matsumura M, 2003. Synergism between rutile and anatase TiO₂ particles in photocatalytic oxidation of naphthalene. *Appl Catal A-Gen*, 244: 383–391.
- Ohno T, Sarukawa K, Tokieda K, Matsumura M, 2001. Morphology of a TiO₂ photocatalyst (Degussa, P-25) consisting of anatase and rutile crystalline phases. *J Catal*, 203: 82–86.
- Ollis D F, 1985. Contaminant degradation in water. *Environ Sci Technol*, 19: 480–484.
- Tang J W, Quan H D, Ye J H, 2007. Photocatalytic properties and photoinduced hydrophilicity of surface-fluorinated TiO₂. *Chem Mater*, 19: 116–122.
- Testino A, Bellobono I R, Buscaglia V, Canevali C, D'Arienzo M, Polizzi S, Scotti R, Morazzoni F, 2007. Optimizing the photocatalytic properties of hydrothermal TiO₂ by the control of phase composition and particle morphology. A systematic approach. *J Am Chem Soc*, 129: 3564–3575.
- Yang J J, Li D X, Zhang Z J, Li Q L, Wang H Q, 2000. A study of the photocatalytic oxidation of formaldehyde on Pt/Fe₂O₃/TiO₂. *J Photoch Photobio A*, 137: 197–202.
- Zhang L W, Fu H B, Zhang C, Zhu Y F, 2006. Synthesis, characterization, and photocatalytic properties of InVO₄ nanoparticles. *J Solid State Chem*, 179: 804–811.
- Zhang H, Banfield J F, 2000. Understanding polymorphic phase transformation behavior during growth of nanocrystalline aggregates: insights from TiO₂. *J Phys Chem B*, 104: 3481–3487.